Velocity selection in coupled-map lattices

Nita Parekh and Sanjay Puri

School of Physical Sciences, Jawaharlal Nehru University, New Delhi 110067, India

We investigate the phenomenon of velocity selection for traveling wave fronts in a class of coupled-map lattices, derived by discretizations of the Fisher equation [Ann. Eugenics 7, 355 (1937)]. We find that the velocity selection can be understood in terms of a discrete analog of the marginal-stability hypothesis. A perturbative approach also enables us to estimate the selected velocity accurately for small values of the discretization mesh sizes.

Much attention has been focused on the problem of propagation of stable states into unstable states [1]. The classic example of such a situation is that of the Fisher equation, which was first proposed as a model of mutant-gene propagation [2]. This equation takes the form (in one dimension)

$$\partial u(x,t)/\partial t = u(x,t)(1-u(x,t)) + [\partial^2 u(x,t)/\partial x^2] , \quad (1)$$

where $u(x,t)$ is a field variable (e.g., order parameter, population density) that depends on space (denoted by x) and time (denoted by t). Kolmogorov, Petrovskii, and Piscounov [2] found that (1) has stable traveling-wave solutions (called "clines"), which are walls traveling in the $+x$ direction with velocity $v \geq 2$ and $u(-\infty,t)=1$, $u(\infty,t)=0$ [or walls traveling in the $-x$ direction with velocity $v \leq 2$ and $u(-\infty,t)=0$, $u(\infty,t)=1$]. Subsequently, Aronson and Weinberger [3] demonstrated the powerful result that a broad class of initial conditions for (1) asymptotically converge to the cline solutions with $v = \pm 2$. In a more general context, Dee and Langer [4] and Ben-Jacob *et al.* [5] studied velocity selection for the propagation of stable states into unstable states and proposed that the selected velocity v^* is such that the front is marginally stable, i.e., front solutions which move slower than v^* are unstable to perturbations (in the comoving frame), while those which move faster than v^* are stable. This hypothesis is supported by results from many partial differential equations, including the Fisher equation [1].

While much attention has been paid to the question of velocity selection in continuous systems (which are described by partial differential equations), there is a paucity of work (with some exceptions [6]) on discrete systems, i.e., coupled-map lattices (CML's) [7] and cellular automata (CA) [8]. However, all numerical implementations of partial differential equations are discrete systems. Furthermore, discrete dynamical systems now constitute an important class of models for real physical phenomena, quite independent of whether or not they are derivable from partial differential equations [7,8]. Thus it is relevant to ask whether there is a velocity selection in discrete systems and, if so, by what mechanism. This is the primary motivation of our study.

In this paper, we address the question of velocity selection for a particular class of CML's which are derived by three different discretization schemes from the Fisher equation. There are two reasons for this choice. First, this class of CML's are extensively studied as dynamical systems in their own right [7]. Second, we are able to understand the velocity-selection behavior as a continuous departure from that of the continuum Fisher equation, for which there already exists a large literature [1]. Our results indicate that these CML's exhibit velocity selection, and this can be understood by a discrete analog of the marginal-stability hypothesis proposed in the context of continuum systems.

There is also a secondary outcome of our study, viz., our results are relevant as an investigation of how the velocity selected in a discrete simulation of a partial differential equation is affected by the mesh sizes and the scheme chosen for the simulation. Typically, if one is interested in simulating a partial differential equation, the merits of a particular numerical scheme are determined by the errors introduced by the scheme, viz., the difference between the true solution of the partial differential equation and the numerical solution obtained. In all the schemes described below, it emerges that the shape of the numerical cline solution matches that of the real cline solution fairly well. The major difference between these schemes lie in the dependence of the velocity selected on the discretization mesh size. This will become clear when we present our results.

Before we proceed, let us return to the continuum equation and explain how one applies the marginal-stability hypothesis to understand velocity selection [1]. Let us look for traveling-wave solutions of (1) with velocity v, i.e., $u(x,t) \equiv u(x-vt) \equiv u(\eta)$, where $\eta = x - vt$. The corresponding equation that must be satisfied by $u(\eta)$ can be cast as the two-dimensional system

$$du(\eta)/d\eta = y(\eta) ,$$
$$dy(\eta)/d\eta = -u(\eta)(1-u(\eta)) - vy(\eta) . \quad (2)$$

The fixed points of this system are $(u^*=0, y^*=0)$ and $(u^*=1, y^*=0)$. If we linearize about the fixed points as $u(\eta)=u^*+\delta u(\eta)$, $y(\eta)=\delta y(\eta)$, we have the linearized system

$$\frac{d}{d\eta} \begin{bmatrix} \delta u(\eta) \\ \delta y(\eta) \end{bmatrix} = \begin{bmatrix} 0 & 1 \\ 2u^*-1 & -v \end{bmatrix} \begin{bmatrix} \delta u(\eta) \\ \delta y(\eta) \end{bmatrix} . \quad (3)$$

It is easy to see that the fixed point $(u^*=1, y^*=0)$ is al-

ways a saddle point, regardless of the value of v. On the contrary, the fixed point $(u^*=0, y^*=0)$ has the eigenvalues $\lambda_\pm = [-v \pm (v^2-4)^{1/2}]/2$ and is always an attractor but has complex eigenvalues for $v<2$ and real eigenvalues for $v \geq 2$. The trajectories that start at $(u^*=1, y^*=0)$ for $\eta = -\infty$ and go to $(u^*=0, y^*=0)$ for $\eta = +\infty$ correspond to the possible wall solutions of (1). Thus the wall solutions for $v<2$ do not decrease monotonically to $u=0$ but rather oscillate about $u=0$. It is easily demonstrated that these oscillatory solutions are unstable [1]. Thus (2) has stable solutions only for the case $v \geq 2$. The velocity $v^*=2$, where a bifurcation in the nature of the fixed point $(u^*=0, y^*=0)$ occurs, also signals the transition from the unstable solutions to the stable solutions. Thus $v^*=2$ is the required marginally stable velocity. From the rigorous results of Aronson and Weinberger [3], we know that this is the selected velocity for a large class of initial conditions on the Fisher equation.

The first CML we will study is the simple one obtained by an Euler discretization of (1), viz.,

$$u(x,t+\Delta t)=u(x,t)+\Delta t u(x,t)(1-u(x,t))$$
$$+\alpha[u(x+\Delta x,t)-2u(x,t)$$
$$+u(x-\Delta x,t)],\qquad (4)$$

where Δt and Δx are, respectively, the mesh sizes in time and space and $\alpha = \Delta t/(\Delta x)^2$. For stability, this explicit scheme must satisfy $\Delta t \leq 2$ and $\alpha \leq (2-\Delta t)/4$ [9]. We have implemented (4) numerically on a one-dimensional lattice with free-end boundary conditions and with initial conditions consisting of (a) step functions of different amplitudes and (b) "tanh" profiles of different widths. All these initial conditions rapidly evolve into a discrete traveling-wave solution with a unique velocity less than 2 and the selected velocity is a function of Δt and α. This velocity selection can be understood from a discrete analog of the argument presented above for the Fisher equation. Let us assume that the discrete lattice points lie on the uniformly translating wave profile $u(x-vt)$ so that (4) becomes

$$u(x-vt-v\Delta t)=u(x-vt)+\Delta t u(x-vt)(1-u(x-vt))$$
$$+\alpha[u(x+\Delta x-vt)-2u(x-vt)$$
$$+u(x-\Delta x-vt)],\qquad (5)$$

where (say) $x=n\Delta x$ and $t=p\Delta t$. We make the further assumption that the velocities can be classified as $v=\Delta x/N\Delta t$, where N is an integer. (This will provide a window in which the selected velocity lies.) Then (5) reduces to the difference equation

$$\psi(m-1)=\psi(m)+\Delta t \psi(m)(1-\psi(m))$$
$$+\alpha[\psi(m+N)-2\psi(m)+\psi(m-N)],\qquad (6)$$

where we have introduced the mapping variable $\psi(m) \equiv u((nN-p)v\Delta t)$. Equation (6) is equivalent to a $2N$-dimensional system of first-order mappings in the variables $\psi(m)$ and $(2N-1)$ difference variables in $\psi(m)$, which we refer to as $\phi_1(m)$ through $\phi_{2N-1}(m)$. The fixed points of this system are $\alpha \equiv [\psi^*=1, \phi_i^*=0$ for

$i=1 \rightarrow (2N-1)]$ and $\beta \equiv [\psi^*=0, \phi_i^*=0$ for $i=1 \rightarrow (2N-1)]$. The trajectory that goes from α for $m=-\infty$ to β for $m=\infty$ corresponds to possible discrete wall solutions. As in the continuum case, the discrete wall solutions that oscillate before settling down to $\psi=0$ are unstable to perturbations. Further, the discrete wall solutions that go monotonically to $\psi=0$ are stable. The corresponding bifurcation for (6) is signaled by the eigenvalues about the fixed point β in the $(\psi(m), \phi_1(m))$ plane [where $\phi_1(m)=\psi(m+1)-\psi(m)$] going from complex attractive to real attractive. The eigenvalues about the fixed point β are easily found by linearizing (6) about $\psi^*=0$ as $\psi(m)=\delta\psi(m)$ and looking for solutions of the form $\delta\psi(m)=\lambda^m$. This yields the eigenvalue equation

$$\alpha\lambda^{2N}+(1+\Delta t-2\alpha)\lambda^N-\lambda^{N-1}+\alpha=0.\qquad (7)$$

We can solve this numerically to find the critical value N^* such that the roots of (7) corresponding to motion in the $(\psi(m), \phi_1(m))$ plane are complex and attractive for $N=N^*$ and real and attractive for $N=N^*+1$. This gives a window inside which the marginally stable velocity must lie, i.e., from $\Delta x/(N^*\Delta t)$, to $\Delta x/(N^*+1)\Delta t$. Figure 1 shows the numerically obtained velocities (marked by asterisks) for the explicit scheme and the window (marked by squares) for the marginally stable velocity for $\alpha=0.1$ and different values of Δt. For very small values of Δt, the windows are far too large and we do not depict them on the figure. From the points shown, it is evident that, for the simple CML considered, our discrete analog of the marginal-stability hypothesis correctly gives a window in which the numerically selected velocity lies.
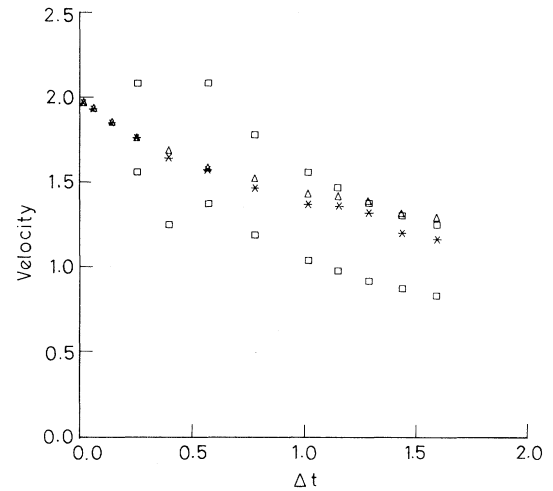

FIG. 1. Results for velocity selection in the CML resulting from an explicit discretization of the Fisher equation. The asterisks denote numerical results on a one-dimensional lattice for a front developing from a range of initial conditions described in the text. The value of α was fixed at 0.1 and free-end boundary conditions were imposed. The velocity is measured at the point where the amplitude of the front is 0.5. The squares denote the velocity window predicted by applying our discrete analog of the marginal-stability hypothesis to the CML. The triangles denote the marginally stable velocity for the partial differential equation resulting from a Taylor expansion to $O(\Delta t^2)$ of the CML equation.

Of course, this window may still be too large to be of practical use. However, our aim is to demonstrate the validity of the discrete marginal-stability hypothesis for CML's rather than to obtain narrow bounds on the selected velocity. Another estimate of the marginally stable velocity for the CML can be obtained by a perturbative expansion of the terms in (4), i.e., replacing the discrete terms by their Taylor expansions in mesh sizes and truncating at a particular order in Δt to obtain a partial differential equation. If the marginal-stability hypothesis is valid, the marginally stable velocity for this equation should approximate the selected velocity for the CML (4) for small values of mesh sizes. Taylor-expanding terms in (4) and retaining only terms to $O(\Delta t^2)$, we obtain

$$\frac{\partial u(x,t)}{\partial t}+\frac{\Delta t}{2}\frac{\partial^2 u(x,t)}{\partial t^2}+\frac{(\Delta t)^2}{6}\frac{\partial^3 u(x,t)}{\partial t^3}$$

$$=u(x,t)(1-u(x,t))+\frac{\partial^2 u(x,t)}{\partial x^2}+\frac{\Delta t}{12\alpha}\frac{\partial^4 u(x,t)}{\partial x^4}$$

$$+[(\Delta t)^2/360\alpha^2][\partial^6 u(x,t)/\partial x^6] . \qquad (8)$$

If we look for traveling-wave solutions of (8), we obtain a system of six first-order differential equations in (u,y_1,y_2,y_3,y_4,y_5), where $y_i(\eta)\equiv d^i u(\eta)/d\eta^i$, $\eta\equiv x-vt$. We study the eigenvalues of this system about the fixed point $(u^*=0,y_i^*=0$ for $i=1\rightarrow5)$. The eigenvalues are given by

$$[(\Delta t)^2/360\alpha^2]\lambda^6+(\Delta t/12\alpha)\lambda^4+[v^3(\Delta t)^2/6]\lambda^3$$

$$+[1-(v^2\Delta t/2)]\lambda^2+v\lambda+1=0 . \qquad (9)$$

As before, the bifurcation of this fixed point from a complex attractor to a real attractor in the (u,y_1) plane signals the marginally stable velocity for the partial differential equation (8). The marginally stable velocity obtained in this fashion is depicted by triangles in Fig. 1. The agreement with numerical results for small and moderate values of Δt is excellent. It is also surprisingly good for large values of Δt but this should be regarded as fortuitous. We remark that the agreement can be improved for all values of Δt by considering higher-order terms in the expansion that led to (8). As a matter of fact, it is possible to retain all orders in perturbation theory but this leads to a transcendental equation for the eigenvalues [10].

Our second example of a CML is obtained by a discretization of the Fisher equation that was proposed by Oono and Puri [11]. In a previous paper [9], we have demonstrated that this scheme enables a reasonable simulation of the Fisher equation at much higher values of Δt (i.e., $\Delta t\geq2$) than are permitted by the explicit scheme. This scheme is of the form

$$u(x,t+\Delta t)=u(x,t)/[u(x,t)+(1-u(x,t))\exp(-\Delta t)]$$

$$+\alpha[u(x+\Delta x,t)-2u(x,t)+u(x-\Delta x,t)] , \qquad (10)$$

where $\alpha=\Delta t/(\Delta x)^2$. This scheme is stable for $\alpha\leq[1+\exp(-\Delta t)]/4$ [9]. Applying the methods described previously, we arrive at the following eigenvalue

equation for determining the window in which the marginally stable velocity lies:

$$\alpha\lambda^{2N}+(e^{\Delta t}-2\alpha)\lambda^N-\lambda^{N-1}+\alpha=0 . \qquad (11)$$

The eigenvalue equation obtained from a perturbative expansion of (10) to $O(\Delta t^2)$ is

$$\frac{(\Delta t)^2}{360\alpha^2}\lambda^6+\frac{\Delta t}{12\alpha}\lambda^4+\frac{v^3(\Delta t)^2}{6}\lambda^3+\left[1-\frac{v^2\Delta t}{2}\right]\lambda^2$$

$$+v\lambda+\{1+(\Delta t/2)+[(\Delta t)^2/6]\}=0 . \qquad (12)$$

Figure 2 shows results for the numerically selected velocity (denoted by asterisks), the window in which the marginally stable velocity lies (denoted by squares), and the marginally stable velocity from a perturbative expansion of (10) (denoted by triangles). Again, we fix $\alpha=0.1$ and vary the value of Δt.

The third (and final) CML we will consider is derived from an implicit discretization of the Fisher equation [12]. The implicit discretization is vastly superior to the explicit discretization as far as numerical stability and numerical errors are concerned. It takes the form

$$u(x,t+\Delta t)=u(x,t)+\Delta t u(x,t)[1-u(x,t)]$$

$$+\alpha[u(x+\Delta x,t+\Delta t)-2u(x,t+\Delta t)$$

$$+u(x-\Delta x,t+\Delta t)] , \qquad (13)$$

so that the diffusion term is discretized at time $t+\Delta t$ rather than at time t. The only requirement for stability of this scheme is that $\Delta t\leq2$.

We can look for discrete traveling-wave solutions of (13) precisely as before. The corresponding eigenvalue equation that emerges for the window in which the marginally stable velocity lies is

$$\alpha\lambda^{2N}+(1+\Delta t)\lambda^{N+1}-(1+2\alpha)\lambda^N-\alpha=0 . \qquad (14)$$

The corresponding eigenvalue equation obtained from the perturbative treatment to $O(\Delta t^2)$ is
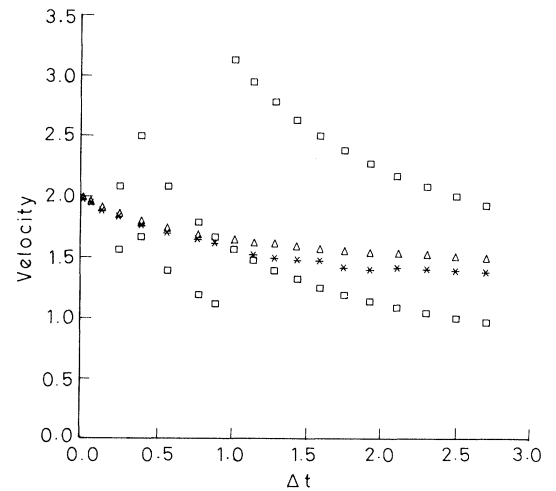

FIG. 2. Results for velocity selection in the CML resulting from the Oono-Puri [11] discretization of the Fisher equation. Numerical results are obtained as described in Fig. 1 and the symbols used have the same meaning as those in Fig. 1.

$$\frac{(\Delta t)^2}{360\alpha^2}\lambda^6 - \frac{v(\Delta t)^2}{12\alpha}\lambda^5 + \frac{\Delta t}{2}\left[v^2\Delta t + \frac{1}{6\alpha}\right]\lambda^4$$

$$+ v\Delta t\left[\frac{v^2\Delta t}{6} - 1\right]\lambda^3 + \left[1 - \frac{v^2\Delta t}{2}\right]\lambda^2 + v\lambda + 1 = 0 \ .$$

$$(15)$$

Figure 3 shows the numerical results (as asterisks) for the selected velocity as a function of Δt for $\alpha = 0.1$. As opposed to the explicit scheme, the velocity remains more or less stable about 2, which is the continuum value, indicating why the implicit scheme is numerically superior to the explicit scheme. Again, the numerical velocity is always inside the window predicted by the marginal-stability approach applied directly to the CML (denoted by squares). The agreement with the marginal-stability hypothesis applied to the perturbatively obtained partial differential equation is rather good, even for large values of Δt (denoted by triangles).

At this stage, it is important to discuss the behavior of the selected velocity as a function of Δt and the implications of this for the numerical merits of the various schemes. For the explicit scheme, the selected velocity decreases rapidly as Δt is increased. Thus, in terms of mimicking the true solution (which has a selected velocity of 2), the explicit scheme is the worst of the three considered here. For the Oono-Puri scheme, the selected velocity again decreases as Δt is increased but not as drastically as for the explicit scheme. Furthermore, the selected velocity saturates out to a steady value (approximately 1.5) at large values of Δt. Finally, the implicit scheme shows steady behavior for the numerically selected velocity, which shows small fluctuations about the value for the continuum Fisher equation. As we have shown elsewhere [9], the shape of the traveling-wave front does not have a strong dependence on the mesh size or the numerical scheme used. Thus the implicit scheme mimicks the true solution best among the schemes considered here. Unfortunately, the implicit scheme is unstable for $\Delta t > 2$, so it cannot be used with very large mesh sizes. Furthermore, the matrix inversion required to apply the implicit scheme is progressively more demanding numerically in
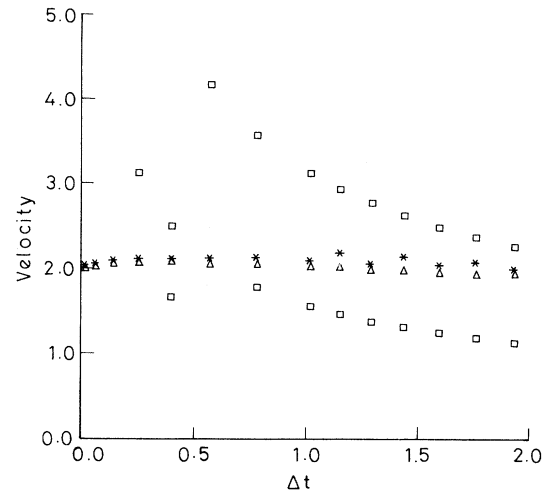

FIG. 3. Results for velocity selection in the CML resulting from an implicit discretization of the Fisher equation. Numerical results are obtained as described in Fig. 1 and the symbols used have the same meaning as those in Fig. 1.

higher dimensions. Our conclusion is that, as far as numerical merits are concerned, the Oono-Puri scheme is the best for dimensions higher than 1. For $d = 1$, one could combine the excellent stability properties of the Oono-Puri scheme (for high values of Δt) with the steady behavior of the selected velocity in the implicit scheme by using a scheme in which the local term is solved exactly (as in the Oono-Puri scheme) and the diffusion term is discretized as in the implicit scheme.

To summarize: We have studied velocity selection in CML's obtained by three different discretizations of the Fisher equation. We find that the numerically selected velocity is in accordance with a discrete analog of the marginal stability hypothesis. We can also obtain a good approximation of the numerically selected velocity for small mesh sizes by applying the marginal-stability hypothesis to the partial differential equations obtained by a Taylor expansion of the CML equations.

[1] W. van Saarloos, Phys. Rev. A 37, 211 (1988); 39, 6367 (1989); and references therein.

[2] R. A. Fisher, Ann. Eugenics 7, 355 (1937); A. Kolmogorov et al., Bull. Univ. Moscow, Ser. Int. Sec. A 1, 1 (1937).

[3] D. G. Aronson and H. F. Weinberger, Adv. Math. 30, 33 (1978); also in Partial Differential Equations and Related Topics, edited by J. A. Goldstein (Springer, Berlin, 1978).

[4] G. Dee and J. S. Langer, Phys. Rev. Lett. 50, 383 (1983).

[5] E. Ben-Jacob et al., Physica D 14, 348 (1985).

[6] M. Bramson et al., J. Stat. Phys. 45, 905 (1986); A. S. Pikovsky, Phys. Lett. A 156, 223 (1991).

[7] For general references on coupled-map lattices, see J. P. Crutchfield and K. Kaneko, in Directions in Chaos, edited

by Hao Bai-Lin (World Scientific, Signapore, 1987), p. 272, and references therein.

[8] For general references on cellular automata, see S. Wolfram, Theory and Applications of Cellular Automata (World Scientific, Singapore, 1986), and references therein.

[9] N. Parekh and S. Puri, J. Phys. A 23, L1085 (1990).

[10] N. Parekh and S. Puri (unpublished).

[11] Y. Oono and S. Puri, Phys. Rev. Lett. 58, 836 (1987); Phys. Rev. A 38, 434 (1988).

[12] W. H. Press et al., Numerical Recipes: The Art of Scientific Computing (Cambridge University Press, Cambridge, England, 1986).